FOXO1 is Required for Binding of PR on *IRF4*, Novel Transcriptional Regulator of Endometrial Stromal Decidualization

Yasmin M. Vasquez, Erik C. Mazur, Xilong Li, Ramakrishna Kommagani, Lichun Jiang, Rui Chen, Rainer B. Lanz, Ertug Kovanci, William E. Gibbons, and Francesco J. DeMayo

Departments of Molecular and Cellular Biology (Y.M.V., X.L., R.K., R.B.L., F.J.D.) and Molecular and Human Genetics (L.J., R.C.), Baylor College of Medicine, and Division of Reproductive Endocrinology and Infertility (E.C.M., E.K., W.E.G.), Department of Obstetrics and Gynecology, Texas Children's Hospital Pavilion for Women, Baylor College of Medicine, Houston, Texas 77030

The forkhead box O1A (FOXO1) is an early-induced target of the protein kinase A pathway during the decidualization of human endometrial stromal cells (HESCs). In this study we identified the cistrome and transcriptome of FOXO1 and its role as a transcriptional regulator of the progesterone receptor (PR). Direct targets of FOXO1 were identified by integrating RNA sequencing with chromatin immunoprecipitation followed by deep sequencing. Gene ontology analysis demonstrated that FOXO1 regulates a subset of genes in decidualization such as those involved in cancer, p53 signaling, focal adhesions, and Wnt signaling. An overlap of the FOXO1 and PR chromatin immunoprecipitation followed by deep sequencing intervals revealed the co-occupancy of FOXO1 in more than 75% of PR binding intervals. Among these intervals were highly enriched motifs for the interferon regulatory factor member 4 (IRF4). *IRF4* was determined to be a genomic target of both FOXO1 and PR and also to be differentially regulated in HESCs treated with small interfering RNA targeting FOXO1 or PR prior to decidualization stimulus. Ablation of FOXO1 was found to abolish binding of PR to the shared binding interval downstream of the *IRF4* gene. Finally, small interfering RNA-mediated ablation of *IRF4* was shown to compromise morphological transformation of decidualized HESCs and to attenuate the expression of the decidual markers *IGFBP1*, *PRL*, and *WNT4*. These results provide the first evidence that FOXO1 is functionally required for the binding of PR to genomic targets. Most notably, FOXO1 and PR are required for the regulation of *IRF4*, a novel transcriptional regulator of decidualization in HESCs. (*Molecular Endocrinology* 29: 421–433, 2015)

Decidualization of the endometrium is a requirement for implantation of the blastocyst and pregnancy progression (1). This highly complex differentiation process involves an extensive transcriptional reprogramming that results in changes in stromal cell morphology, steroid responsiveness, secretory profile, resistance to oxidative stress, and extracellular matrix remodeling (2). The decidua provides critical histiotrophic support for the developing embryo and modulates the maternal immune system for tolerance of the fetal allograft (3). Decidualization occurs in the secretory phase of the menstrual cycle under the control of the ovarian steroid hormones estradiol and progesterone (4). Progesterone acts via its cognate nuclear receptor, the progesterone receptor (PR) to regulate the expression of numerous effectors of the differentiation of endometrial stromal cells (5, 6).

Abbreviations: CEBP, CCAAT/enhancer-binding protein; ChIP-qPCR, chromatin immunoprecipitation-quantitative PCR; ChIP-seq, chromatin immunoprecipitation followed by deep sequencing; DAVID, Database for Annotation, Visualization, and Integrated Discovery; EPC, 2′-O-dibutyryladenosine-3′, cAMP; FOXO1, forkhead box O1A; HESC, human endometrial stromal cell; HOXA, homeobox A; IGFBP, IGF binding protein; IRF4, interferon regulatory factor member 4; ISRE, interferon-stimulated response element; PEM, potassium 1,4-piperazine diethane sulfonic acid, EGTA, and $MgCl_2$; PKA, protein kinase A; PR, progesterone receptor; PRE, progesterone response element; PRL, prolactin; RNA-seq, RNA sequencing; RNApol II, RNA polymerase II; RT-qPCR, reverse transcription real-time quantitative PCR; RUNX, Runt-related transcription; siFOXO1, FOXO1-targeting siRNA; siIRF4, IRF4-targeting siRNA; siNT, nontargeting siRNA; siRNA, small interfering RNA; UTR, untranslated region.

Along with steroid signaling, it has been shown that decidualization of stromal fibroblasts depends on cAMP stimulation and sustained activity of the downstream protein kinase A (PKA). The PKA pathway integrates the progesterone input by sensitizing cells for progesterone action and enhancing the transcriptional activity of PR. Activation of the PKA pathway disrupts the interaction of PR with the corepressors nuclear receptor corepressor and silencing mediator of retinoid and thyroid receptors, facilitates recruitment of the coactivator nuclear receptor coactivator 1, and attenuates the inhibitory SUMOylation of PR (7–9). The PKA pathway also induces the expression of diverse transcription factors capable of modulating PR function, including signal transducer and activator of transcription-5, CCAAT/enhancer-binding protein (CEBP)-β, and forkhead box O1A (FOXO1) (10). FOXO1 is an early-induced target of cAMP that has long been used as a marker of decidualization in human endometrial stromal cell (HESC) differentiation. FOXO1, like other members of the Forkhead transcription factor subclass, regulates genes involved in cell cycle inhibition, DNA repair, resistance to oxidative stress, and apoptosis, all of which are critical aspects of decidualization (11, 12). Moreover, FOXO1 was identified to regulate a subset of decidual genes including *IGFBP1*, *PRL*, *DCN*, and *TIMP3* in HESCs (13). FOXO1 has been described as a transcriptional coregulator of PR during decidualization with in vitro evidence suggesting there is a direct physical interaction between PR and FOXO1 (14). The role of FOXO1 as a transcriptional coregulator of CEBP-β, and homeobox A (HOXA)-11 has been clearly demonstrated by its ability to cooperatively activate the prolactin (PRL) promoter in luciferase reporter assays (15, 16). Additionally, PR, FOXO1, CEBP-β, and HOXA10 are also involved in the transcriptional regulation of the IGF binding protein (IGFBP)-1 promoter (17–19). However, the direct genomic targets of FOXO1 on a global scale and the requirement of the FOXO1/PR interaction for the regulation of transcription during decidualization remain to be determined.

In this study, we aimed to determine the transcriptional role of FOXO1 in stromal cell differentiation. For this purpose we used primary HESCs isolated from healthy proliferative phase biopsies and cultured them under a well-defined hormone regimen for the induction of decidualization (20). This cell based system is currently the most reliable and clinical translatable method to interrogate the molecular mechanisms underlying decidual transformation of the endometrial stromal compartment during the secretory phase of the menstrual cycle in preparation for pregnancy (21, 22). To better elucidate the role of FOXO1 in endometrial stroma cell biology, we implemented a small interfering RNA (siRNA)-mediated loss of function approach and defined the FOXO1-dependent transcriptome by RNA sequencing (RNA-seq). The direct targets of FOXO1 in decidualizing HESCs were defined by integrating RNA-seq with chromatin immunoprecipitation followed by deep sequencing (ChIP-seq). Furthermore, we compared the FOXO1 binding profile with that of PR and identified potential genes the expression of which is modulated by both FOXO1 and PR. We then determined the requirement of FOXO1 for the PR-dependent expression of *IRF4* and identified interferon regulatory factor member 4 (IRF4) as a critical transcriptional regulator of HESC decidualization.

Materials and Methods

Primary human endometrial cell culture

HESCs were obtained from healthy, reproductive-aged volunteers with regular menstrual cycles and no history of gynecological malignancies under a human subject protocol approved by the Institutional Review Board of Baylor College of Medicine. An endometrial biopsy was performed during the proliferative phase of the menstrual cycle (cycle d 7–12). The HESC cultures were established as previously described (20). Briefly, tissue biopsies were washed twice with Hanks' balanced salt solution containing 100 U/mL penicillin and 100 μg/mL streptomycin and mechanically digested for 20 minutes. Minced tissue was centrifuged to remove media and incubated with 25 mg collagenase (C-130; Sigma) and 5 mg deoxyribonuclease I (DN25; Sigma) dissolved in 10 mL of DMEM F12 with antibiotics and antimycotic and filtered through a 0.2-μm filter for 90 minutes in a 37°C water bath and vortex every 10 minutes. The digested sample was filtered using a 40-μm filter. Stromal cells that flowed through the filter were pelleted by centrifugation and washed with 10 mL DMEM F12 media with antibiotic-antimycotic. The stromal cells were subsequently cultured in HESC media (DMEM F12, 10% fetal bovine serum, antibiotic-antimycotic, HEPES, and NaHCO$_3$). Experiments were carried out in HESCs cultured in fewer than four passages.

siRNA transfection and in vitro decidualization

When cells reached approximately 70% confluence, they were transfected with 60 nM scrambled, nontargeting siRNA (siNT), FOXO1-targeting siRNA (siFOXO1), PR-targeting siRNA, or IRF4-targeting siRNA (siIRF4) (ON-TARGET*plus*; Thermo Scientific) using Lipofectamine RNAiMax lipid (Life Technologies) per the manufacturer's instructions. After 48 hours of transfection exposure, cells were either collected as day 0 or exposed to 10 nM 17β-estradiol, 100 nM medroxyprogesterone acetate, and 1 mM 2′-O-dibutyryladenosine-3′, cAMP (DO627; Sigma), herein referred to as EPC, in OPTI-MEM I (Invitrogen) reduced serum media supplemented with 2% stripped fetal bovine serum and antibiotic and antimycotics for 3 or 6 days with the media and hormone replenished every 48 hours.

RNA isolation, RT-PCR, and quantitative PCR

Reverse transcription real-time quantitative PCR (RT-qPCR) was performed to validate RNA-seq gene expression targets. mRNA was isolated by TriZOL (Life Technologies) extraction per the manufacturer's protocol from independent patient samples of transfected siRNA and treated with hormones as described above. RNA was reverse transcribed into cDNA with Moloney murine leukemia virus (Life Technologies) according to the manufacturer's recommendations. Expression levels of mRNA were determined by RT-qPCR on a QuantStudio 12K Flex real-time quantitative PCR system (Life Technologies) using FastStart SYBR Green Master (Roche Diagnostics) and oligonucleotide primers synthesized by Sigma-Aldrich based on sequences deposited in the PrimerBank (23). Gene expression was normalized to 18s rRNA.

RNA sequencing

RNA was purified from three patient samples for RNA-Seq analysis using the Ambion RiboPure kit (Life Technologies). RNA-Seq was performed for each individual patient samples. Raw reads were mapped to human genome hg19 and splice junction sites with Bowtie (version 0.12.7) (24) and TopHat (version 2.0.0) (25) with the strand-specific model that matches the deoxyuridine 5-triphosphate library construction protocol (26). The human annotation file was downloaded from the University of California, Santa Cruz (http://genome.ucsc.edu/). Read counts for each gene were calculated by HTSeq (http://www.huber.embl.de/users/anders/HTSeq/doc/overview.html) using the default model. Differential gene expression was then analyzed with R (version 2.14.0) and the Bioconductor edgeR package (edgeR_2.4.6) (27). With edgeR, we fit a negative binomial generalized log-linear model to the read counts for each gene by accounting for both patient and treatment in the design. We then conducted statistical tests to identify genes that had consistent changes in response to treatment across three patients. A false discovery rate of 0.05 was used as the cutoff for significant differential expression.

Chromatin immunoprecipitation followed by deep sequencing

ChIP-seq for RNA polymerase II (RNApol II) and FOXO1 were performed by Active Motif, Inc on HESCs isolated from proliferative-phase endometrial biopsy specimens and decidualized with EPC for 72 hours. HESCs were fixed with formaldehyde, permeabilized with Igepal CA-630 (number I-8896; Sigma), washed with PBS containing 1 mM phenylmethanesulfonyl fluoride (number P-7626; Sigma), snap frozen, and shipped on dry ice. The six independent patient samples were pooled for sonication. DNA library generation was performed by Active Motif as previously described (28). DNA library sequencing and mapping to the human genome (GRCh Build 37; February 2009) was performed as previously described (29). Associated genes were called if FOXO1 intervals were located within ± 10 kb of the gene boundaries.

Chromatin immunoprecipitation-quantitative PCR (ChIP-qPCR)

HESCs were treated with EPC for 3 days to stimulate a decidual response as described above. One hour before fixation treatment, fresh media with decidualizing agents were replen-

ished. Formaldehyde-assisted chromatin fixation, chromatin preparation, sonication, and immunoprecipitation were performed using the high-sensitivity ChIP-It kit and the EpiShear probe sonicator from Active Motif as per the manufacturer's instructions. Immunoprecipitation reactions were performed with antibodies for FOXO1 (sc-11350), PR (sc-7208), and IgG (sc-2027) (Santa Cruz Biotechnology, Inc). Primers were designed to span the genomic region containing the highest signal intensity for FOXO1 and PR peaks (Supplemental Table 3). The input chromatin was used to generate a standard curve for the amplification of each primer set to determine the amount of DNA immunoprecipitated by IgG, PR, and FOXO1 antibodies. Binding data were represented as the fold enrichment over the Human Negative Control Primer Set 2 (catalog number 71002; Active Motif) or a percentage of the input.

Western blot analysis of protein expression

Parallel samples for HESCs transfected with siNT and siFOXO1 and treated with vehicle or EPC were harvested for Western blot detection of protein expression. Cells were washed and scraped with protein lysis buffer (10 mM Tris, pH 7.4; 150 mM NaCl; 2.5 mM EDTA; and Nonidet P-40) supplemented with protease inhibitor cocktail (cOmplete Mini, EDTA free, reference number 11–836-170–001; Roche Diagnostics) and phosphatase inhibitor cocktail (PhosSTOP, reference number 04–906-837–001; Roche Diagnostics). For the Western blot analysis of FOXO1 cellular localization, decidual HESC nuclear and cytoplasmic fractions were isolated with the universal co-immunoprecipitation kit as per the manufacturer's instructions (catalog number 54002; Active Motif). Denatured protein extracts (10 μg) per sample were loaded on a Bis-Tris NuPAGE 4%–12% (reference number NP0321BOX; Novex by Life Technologies) for electrophoresis separation. Proteins were transferred to polyvinylidene difluoride membranes (Millipore Corp) in transfer buffer (25 mM Tris, 192 mM glycine, and 20% methanol) (Life Technologies). Polyvinylidene difluoride membranes were subsequently blocked with 5% blotting grade nonfat milk (number 170–6404; Bio-Rad Laboratories) in PBS containing 0.1% Tween 20 for 1 hour at room temperature. Membranes were probed with antibodies for PR (sc-7208; Santa Cruz Biotechnology), FOXO1 (number 2880; Cell Signaling), glyceraldehyde-3-phosphate dehydrogenase (number 2118; Cell Signaling), Lamin A/C (number 2032; Cell Signaling), and β-actin (catalog number A5441; Sigma-Aldrich) overnight at 4°C in 5% blotting grade nonfat milk in PBS buffer containing 0.1% Tween 20. Blotted membranes were subsequently washed three times with PBS containing 0.1% Tween 20 and incubated 1 hour at room temperature with a secondary antibody (antirabbit peroxidase and antimouse peroxidase, accordingly). Blots were washed three times with PBS containing 0.1% Tween 20 and an additional three times with PBS only. The Amersham ECL Western blotting system (GE Healthcare) was used for the luminol-based detection of bands on film as per the manufacturer's instructions.

Confocal immunofluorescence imaging of FOXO1

HESCs were grown on coverslips and treated with EPC for 3 days to stimulate a decidual response as described above. One hour before the fixation treatment, fresh media with decidualizing agents were replenished. HESCs were washed with PBS

and fixed with 4% formaldehyde in buffer of potassium 1,4-piperazine diethane sulfonic acid (pH 6.8), 5 mM EGTA (pH 7.0), and 2 mM $MgCl_2$ (PEM) for 30 minutes and subsequently washed three times with PEM alone. Autofluorescence was quenched with 1 M ammonium chloride diluted 1:10 in PEM for 10 minutes and subsequently washed twice with PEM. HESCs were permeabilized with PEM + 0.5% Triton X-100,

washed three times with PEM, and blocked with 5% powdered milk in Tris-buffered saline and 0.1% Tween 20 buffer plus 0.02% sodium azide for 1 hour. Blocking buffer was removed and HESCs were incubated with the FOXO1 antibody (number 2880; Cell Signaling) diluted 1:300 overnight at 4°C. After four washes with blocking buffer, HESCs were incubated with Alexa Fluor-conjugated (A546; Life Technologies) secondary anti-
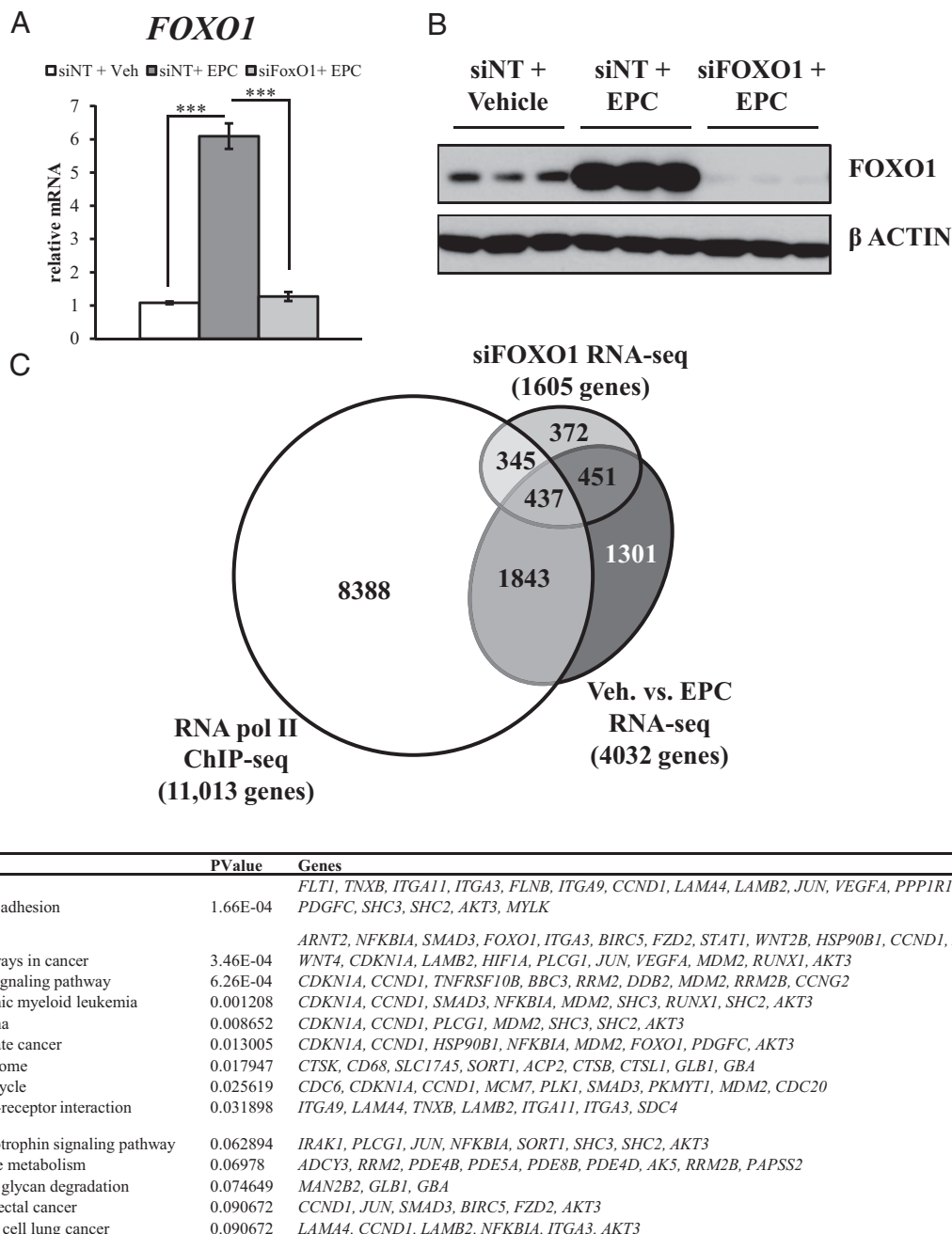
Figure 1. Identification of actively transcribed FOXO1 and decidual target genes in HESCs by RNA-seq and ChIP-seq. A, HESCs transfected with scrambled siRNA (siNT) and targeting siRNA (siFOXO1) prior to treatment with vehicle (Veh) or EPC decidual stimulus. Gene expression validation of *FOXO1* by RT-qPCR and normalization with 18s rRNA. Data are based on three independent experiments. Error bars represent SEM (one-way ANOVA; $P < .0001$). Tukey-Kramer multiple comparisons test included siNT+Veh and siNT+EPC ($P < .0001$), siNT+EPC and siFOXO1+EPC (***, $P < .0001$), siNT+Veh and siFOXO1+EPC ($P > .05$). B, Western blot analysis of FOXO1 and β-actin in HESCs transfected with siNT or siFOXO1 prior to treatment with vehicle or EPC decidual stimulus. C, Venn diagram comparison of genes regulated in HESCs treated with EPC, genes regulated in HESCs transfected with siRNA targeting *FOXO1* prior to EPC treatment, and genes with RNApol II binding in EPC-treated HESCs. D, DAVID pathway analysis of RNApol II bound, vehicle, and EPC-regulated and siFOXO1-regulated genes.

body (1:5000 dilution) for 1 hour at room temperature protected from light. HESCs were washed four times with PEM, incubated 15 minutes with 4% formaldehyde in PEM, washed three times with PEM, and subsequently incubated with PEM + 1 mg/mL NaBH$_4$ to postfix autofluorescence quenching. DNA was counterstained with 4′,6′-diamino-2-phenylindole and subsequently washed with Tris-buffered saline and 0.1% Tween 20. Coverslips were mounted on slides with SlowFade Gold (catalog number S-2828; Molecular Probes). Images were acquired using a GE Healthcare Deltavision image restoration microscope with a ×20/0.75 NA objective. The 0.35-mm optical sections (z-stacks) were taken, deconvolved using the SoftWorx software, and the maximum intensity projected.

Data analysis

Sequence conservation, analysis of enriched motifs (SeqPos), and CEAS enrichment on chromosome and annotation were performed using the Cistrome Analysis Pipeline software (http://cistrome.org/ap/) under the default settings (30). The public Database for Annotation, Visualization, and Integrated Discovery (DAVID; http://david.abcc.ncifcrf.gov/) was used for gene functional classifications running the default settings (31). Statistical analysis of gene expression changes by RT-qPCR and of binding by ChIP-qPCR was performed with GraphPad InStat version 3.06. One-way ANOVA was followed with Tukey-Kramer multiple comparisons test, where appropriate.

Results

FOXO1 regulation of decidual genes

To evaluate the role of FOXO1 in the regulation of decidual genes, HESCs were transfected with scrambled siRNA (siNT) or siRNA targeting *FOXO1* (siFOXO1). After 48 hours of knockdown, the siNT-transfected HESCs and siFOXO1-transfected HESCs received treatment with a decidualizing hormone regimen containing estrogen, medroxyprogesterone, and cAMP (EPC) for 72 hours. In parallel, a cohort of siNT-transfected cells received vehicle treatment. As shown in Figure 1A, FOXO1 was induced at the mRNA level upon EPC treatment of HESCs transfected with siNT. Transfection of HESCs with siFOXO1 abolished this induction to the level of *FOXO1* expression in HESCs transfected with siNT and treated with vehicle. Western blot analysis of protein expression determined that FOXO1 was robustly induced in the siNT + EPC treatment compared with the siNT + vehicle treatment. FOXO1 expression was abolished in the siFOXO1 + EPC treatment (Figure 1B). Immunolocalization of FOXO1 was identified in the nucleus and cytoplasm of decidual HESCs (Supplemental Figure 1A). Cellular fractionation indicated most FOXO1 was found in the cytoplasm, with a residual nuclear fraction (Supplemental Figure 1B). We then performed RNA-seq on these samples and compared differentially expressed genes between siNT + vehicle and siNT + EPC (RNA-seq

vehicle and EPC) and between siNT + EPC and siFOXO1 + EPC (RNA-seq siFOXO1).

To determine which genes were actively being transcribed at the time of cell harvesting of EPC-treated HESCs, we also performed ChIP-seq for RNApol II. RNApol II ChIP-seq identified 11 013 genes containing RNApol II binding intervals within the gene body. Figure 1C is a Venn diagram of the regulated genes with EPC treatment (4032 genes), siFOXO1 (1605 genes) and genes bound by RNApol II (Supplemental Table 1). From this analysis we determined that at least 437 genes were actively being transcribed, as indicated by the occupancy of RNApol II and regulated by FOXO1 in a decidualizing context. Among the EPC-regulated genes that were differentially regulated with FOXO1 knockdown were the canonical markers of decidualization *IGFBP-1* and *PRL* (Supplemental Figure 2). DAVID analysis revealed that these 437 genes enriched biological themes for focal adhesion, pathways in cancer, and p53 signaling (Figure 1D). DAVID gene ontology terms are summarized in Supplemental Table 2.

Evaluation of FOXO1-binding sites in decidualized HESCs

To describe the global binding of FOXO1 and identify the direct genomic targets, ChIP-seq for FOXO1 was per-
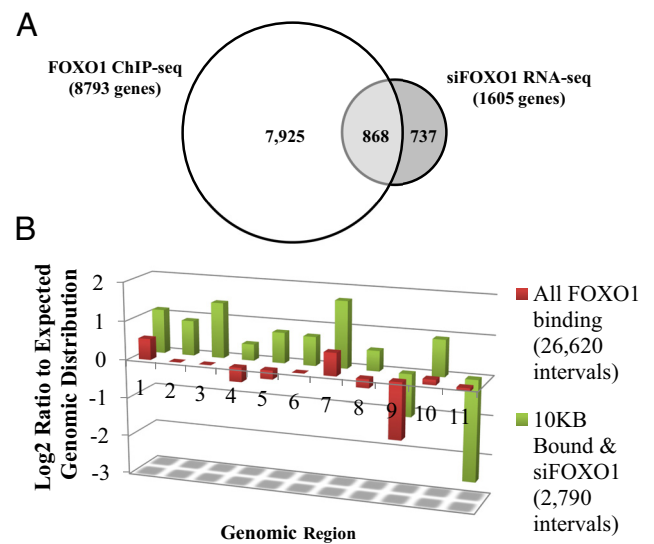

Figure 2. Genomic Enrichment of FOXO1 binding intervals. A, Venn diagram comparing the annotation of FOXO1 genomic binding within 10 kb of genomic boundary of 8793 genes and the genes regulated in HESCs transfected with siRNA targeting FOXO1 prior to EPC treatment. B, CEAS enrichment analysis of FOXO1 genomic binding represented as log2 ratio to the expected genomic distribution. Red bar shows all 26 620 binding intervals of FOXO1 in the genome, and green bars show the enrichments of intervals within 10 kb of genomic boundaries of differentially regulated in HESCs transfected with siRNA targeting FOXO1 prior to EPC stimulus. Genomic region included the following: 1) promoter (≤1000 bp); 2) promoter (1000–2000 bp); 3) promoter (2000–3000 bp); 4) downstream (≤1000 bp); 5) downstream (1000–2000 bp); 6) downstream (2000–3000 bp); 7) 5′UTR; 8) 3′UTR; 9) coding exon; 10) intron; and 11) distal intergenic.

formed after a 72-hour in vitro decidualization of HESCs. The binding of FOXO1 was defined to 26 620 genomic intervals. By CEAS enrichment analysis, these intervals showed no significant enrichments for specific genomic boundaries relative to the genome reference (Figure 2B.) However, we observed an enrichment in the promoter (2000–3000 bp) and 5′-untranslated region (UTR) regions in FOXO1-intervals that were found within 10 kb of genes that were differentially regulated in HESCs transfected with siRNA targeting FOXO1 (2790 intervals).

Gene ontology and pathway analysis tools in DAVID were used to further annotate the FOXO1-dependent genes that are bound by FOXO1 within 10 kb of genomic boundaries. This analysis revealed that a predominance of FOXO1-regulated genes is involved in pathways previously associated with the FOX protein family. Among these pathways were cancer, p53 signaling, focal adhesions, and Wnt signaling (Table 1). However, within these known pathways were previously unidentified components. Ablation of FOXO1 resulted in the up-regulation of several genes that are normally down-regulated in the differentiation of HESCs, including *PDGFC*, *MDM2*, *ROCK2*, *WNT2B*, *FAS*, and *CDKN1A*. Silencing of FOXO1 also attenuated the expression of genes induced in decidualization including *ITGA4*, *ZEB1*, *WNT2*, *HGF*, *CXCL12*, *FLT1*, and *VCAN*. Of note is the enrichment in genes involved in the chemokine signaling pathway (eg, *ROCK2*, *NFKBIA*, *CCL8*, and *CXCL12*) and

cell adhesion molecules (eg, *ITGA4* and *VCAN*) (Supplemental Figure 2).

Validation of direct targets of FOXO1 in decidualization

We followed this analysis with the validation of FOXO1 ChIP-seq binding sites by ChIP-qPCR. Figure 3A represents the binding of FOXO1 to target genomic locations as fold enrichment over the binding of FOXO1 to a gene desert region in chromosome 4 and normalized to the enrichment of the IgG immunoprecipitated DNA. We used RT-qPCR to validate known and putative novel FOXO1-dependent genes that are bound by FOXO1 in decidualization. *FOXO1* knockdown resulted in the up-regulation of the proproliferative genes *CDK1* and *RUNX1* and inhibited the expression of *HIF1A*, *RUNX2*, *CAMKK1*, *AXIN2*, *CEBPA*, and *IGF1*. This evidence suggests that the binding of FOXO1 in proximity to genomic boundaries can have inhibitory or stimulatory effects on the transcriptional activity of genes that are themselves key effectors in the morphological and secretory transformation of the stroma.

Identification of cooperative factors of FOXO1

FOXO1-binding intervals were evaluated for enriched motifs using the SeqPos tool in Cistrome (Supplemental Table 4). The most enriched motifs were those recognized by members of the forkhead domain family followed by

Table 1.   DAVID Pathway Analysis of FOXO1-Bound and siFOXO1-Regulated Genes

Term	Genes
Pathways in cancer	*ARNT2, MITF, NFKBIA, FOXO1, GLI3, PTEN, MMP2, ARNT, WNT2, WNT4, BCL2, FAS, RUNX1, AXIN2, AKT3, CEBPA, AR, PLD1, EPAS1, SMAD3, IGF1, ITGA3, SMAD2, HGF, STAT1, COL4A6, WNT2B, FZD6, JUP, CDKN1A, LAMA4, HIF1A, JUN, NTRK1, MDM2*
Focal adhesion	*CAV2, TNXB, FLT1, ROCK2, ITGA11, IGF1, ITGA3, ITGA4, HGF, PTEN, FLNB, COL4A6, ITGA9, LAMA4, ITGB8, RASGRF1, JUN, BCL2, PDGFC, SHC3, MYLK, AKT3, SHC4*
O-glycan biosynthesis	*GALNT10, GALNT7, WBSCR17, GALNTL2, GCNT1, C1GALT1, GALNT13*
Axon guidance	*PLXNC1, ROCK2, PLXNA2, ABLIM3, CXCL12, NTN1, EPHA2, SEMA5A, SEMA6D, SEMA3C, EFNA5, SEMA3A, UNC5C, PPP3CA, SRGAP1*
ECM-receptor interaction	*ITGA9, LAMA4, SDC1, TNXB, CD44, ITGB8, ITGA11, ITGA3, ITGA4, SDC4, COL4A6*
HCM	*ITGA9, ACE, ITGB8, DMD, PRKAG2, ITGA11, IGF1, CACNB3, ITGA3, ITGA4, CACNA2D3*
ARVC	*JUP, ITGA9, ITGB8, DMD, ITGA11, CACNB3, ITGA3, ITGA4, CDH2, CACNA2D3*
p53 signaling pathway	*CDK1, CDKN1A, BBC3, DDB2, MDM2, IGF1, FAS, GADD45A, PTEN*
ABC transporters	*ABCA8, ABCA9, ABCA1, ABCA4, ABCG1, ABCA6, ABCA13*
Wnt signaling pathway	*PPP2R1B, ROCK2, PPP2R5A, SMAD3, SMAD2, DAAM1, FZD6, WNT2B, WNT2, WNT4, JUN, PPP2CB, PPP3CA, AXIN2, PLCB1*
Prostate cancer	*CDKN1A, AR, BCL2, NFKBIA, MDM2, IGF1, FOXO1, PDGFC, PTEN, AKT3*
Dilated cardiomyopathy	*ADCY3, ITGA9, ITGB8, DMD, ITGA11, IGF1, CACNB3, ITGA3, ITGA4, CACNA2D3*
Chemokine signaling pathway	*ADCY3, ROCK2, PREX1, NFKBIA, CCL8, GNG12, STAT1, CXCL12, DOCK2, TIAM2, GNG2, JAK2, PLCB1, SHC3, AKT3, SHC4*
Melanoma	*CDKN1A, MITF, MDM2, IGF1, PDGFC, HGF, PTEN, AKT3*
TGF-β signaling pathway	*PPP2R1B, ROCK2, ID1, PPP2CB, SMAD3, SMAD2, DCN, ID3, BMP8A*
CAMs	*PVR, ITGA9, SDC1, PTPRM, NRXN3, ITGB8, CNTN1, VCAN, CLDN11, ITGA4, CDH2, SDC4*

Abbreviations: ABC, ATP-binding cassette; ARVC, arrhythmogenic right ventricular cardiomyopathy; CAM, cell adhesion molecule; HCM, hypertrophic cardiomyopathy. The Kyoto Encyclopedia of Genes and Genomes pathway was enriched in genes bound and regulated by FOXO1 (868 genes).
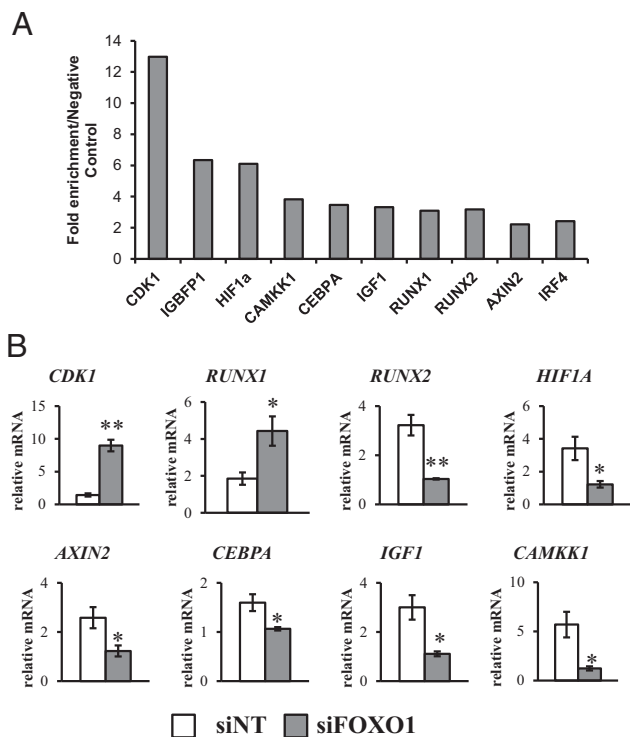
Figure 3. Direct targets of FOXO1 in HESC decidualization. A, ChIP-RT-qPCR validation of FOXO1 binding near genes regulated by FOXO1. Data are represented as fold enrichment of FOXO1 binding over that of the negative control region in a gene desert on chromosome 4. B, HESCs transfected with scrambled siRNA (siNT) and targeting siRNA (siFOXO1) prior to treatment with decidual stimulus. Gene expression validation by RT-qPCR of genes enriched in a pathway analysis. Data for each gene were normalized to that of 18s rRNA. Data are based on three independent experiments. Error bars represent SEM. *, $P < .05$; **, $P < .01$; ***, $P < .001$.

motifs recognized by the leucine zipper family (basic leucine zipper domain), Runt domain family, high-mobility group, homeodomain, and helix-loop-helix factors (basic helix loop helix) (Table 2). Of particular interest was the presence of the half progesterone response element (PRE) under the nuclear hormone receptor family. Previous data from our laboratory identified an enrichment of forkhead domain family motifs in the PR cistrome (our unpublished data). The presence of PRE within the FOXO1-binding intervals and Forkhead response elements within the PR-binding intervals supports the hypothesis that FOXO1 and PR may be binding near each other to regulate decidual transcription.

We pursued this evidence with a comparison of the FOXO1 and PR ChIP-seq data sets. Figure 4A represents the co-occupancy of FOXO1 and PR in the genome in EPC-treated HESCs, in which approximately 75% of the PR genomic binding intervals also contain FOXO1 binding. The FOXO1 and PR intervals were overlaid to generate chromosomal coordinates for the genomic regions of FOXO1 and PR co-occupancy. These chromosomal
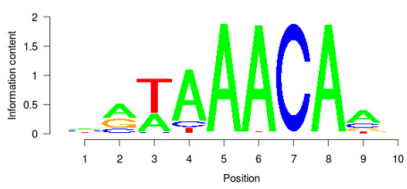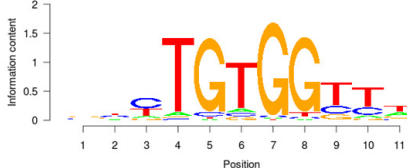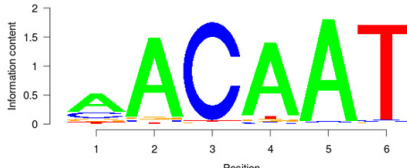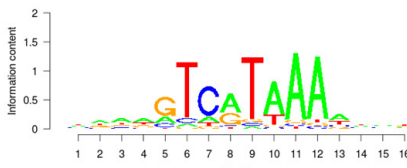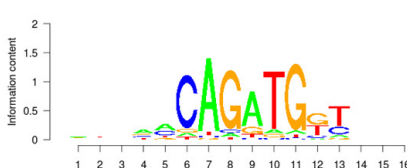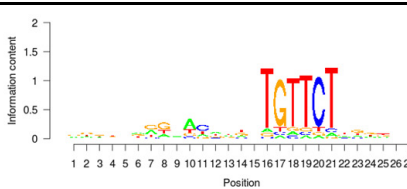
coordinates were submitted to Cistrome for SeqPos motif analysis (Supplemental Table 5). The most enriched motif family in these intervals was that of the hormone-nuclear receptor family, which included the full palindromic PRE (Figure 4B). Among the other enriched motifs recognized by the leucine zipper family, the forkhead domain family, the homeodomain family, and the interferon regulatory factor. Representative PSSM graphs for the forkhead response element and the interferon-stimulated response element (ISRE) are shown in Figure 4B. Further analysis of the FOXO1 and PR co-occupied intervals was performed with the CEAS module in Cistrome. The FOXO1/PR interval distribution was calculated as a log2 ratio relative to genomic distribution. This analysis revealed that the enrichment pattern of the FOXO1 and PR intervals mirrors the enrichment pattern of the total PR intervals (Figure 4C).

Identification of IRF4 as a direct target of FOXO1 and PR

We followed the analysis of FOXO1 and PR co-occupied intervals by identifying unique genes containing FOXO1/PR-binding sites within 10 kb of gene boundaries. The analysis identified 3037 genes, of which 236 genes showed differential regulation in HESCs transfected with PR targeting siRNA and siFOXO1 (Supplemental Table 6). Ontology analysis of these genes revealed an enrichment of genes involved in vasculature development, cell adhesion, response to organic substance, cell motion, and the enzyme-linked receptor protein signaling pathway (Supplemental Table 7).

From this analysis we identified two intervals co-occupied by PR and FOXO1 downstream of *IRF4* (Figure 5A). We sought to determine the requirement of FOXO1 for binding of PR to the most proximal downstream interval on *IRF4*. HESCs were treated with scrambled siRNA (siNT) or siRNA targeting FOXO1 (siFOXO1) prior to decidual stimulation with EPC. Western blot analysis of protein expression revealed that the efficient ablation of FOXO1 in the siFOXO1-treated cells did not affect the levels of either PR isoform (Figure 5B). In HESCs transfected with siNT, PR exhibits robust fold enrichment on *IRF4* over the negative control region. This enrichment was absent in HESCs transfected with siRNA targeting FOXO1 (Figure 5C). The assay was repeated on the more distal shared interval and produced identical results (data not shown). Furthermore, ablation of either FOXO1 or PR in HESCs prior to EPC stimulus is sufficient to inhibit the normal induction of IRF4 during decidualization (Figure 5D). These data suggest that binding of PR on *IRF4* requires FOXO1 and that binding of these factors on *IRF4* is required for the normal transcription of the *IRF4* during the decidualization of HESCs. The FOXO1-dependent binding

Table 2.   Enriched Motifs in FOXO1-Binding Intervals

DNA-binding Domain Family	Motif Example	Factors
Forkhead Domain Family	**FOXO1**	FOXO3, FOXO4, FOXD1, FOXA1, FOXA2
Leucine zipper Family (bZIP)	**JUN**	AP-1, FOS, FOSB, JUN, JUNB, JUND, BACH2, GNC4, CEBPA
Runt Domain Family	**RUNX1**	RUNX2, RUNX3, PEBP1
High Mobility Group	**SOX17**	SOX5, SRY, SOX2, ROX1, SOX10
Homeodomain Family	**HOXA11**	HOXC10, HOXC11, HOXD11, HOXA13, HOXA9
Helix-loop-helix factors (bHLH)	**TCF3**	TCF4, NEUROD1
Hormone-nuclear Receptor Family	**PGR**	NR1H4, RORB, NR2F2, AR, PPARA, ESR1, NR3C1

Abbreviations: bHLH, basic helix loop helix; bZIP, basic leucine zipper domain. Chromosome location coordinates of FOXO1 binding intervals were analyzed with the SeqPos tool in Cistrome.
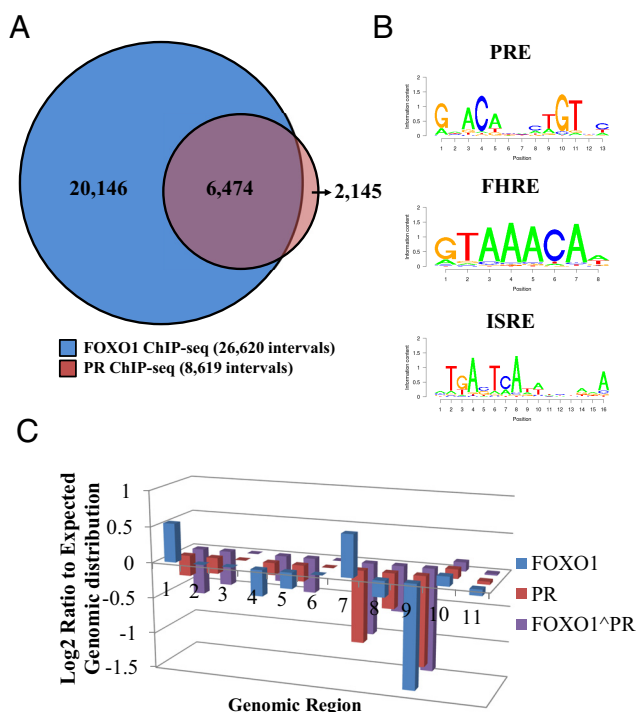
Figure 4. Shared FOXO1 and PR cistrome in decidualized HESCs. A, Venn diagram comparing the genomic binding of FOXO1 and PR. B, Representative Progesterone Response Elements (PRE), Forkhead response elements (FRE), and Interferon-stimulated Response Element (ISRE) identified by SeqPos motif enrichment analysis of the shared FOXO1/PR binding intervals. C, CEAS enrichment analysis of FOXO1, PR, and FOXO1/PR co-occupied genomic binding represented as log2 ratio to the expected genomic distribution. Genomic regions included the following: 1) promoter (≤1000 bp); 2) promoter (1000–2000 bp); 3) promoter (2000–3000 bp); 4) downstream (≤1000 bp); 5) downstream (1000–2000 bp); 6) downstream (2000–3000 bp); 7) 5′UTR; 8) 3′UTR; 9) coding exon; 10) intron; and 11) distal intergenic.

of PR to additional shared targets was also evaluated. Ablation of FOXO1 completely abolished PR binding on *CDK1* and *IGF1*. Interestingly, on targets such as *ZEB1* and *KLF15*, the ablation of FOXO1 significantly attenuated but did not abolish PR binding (Supplemental Figure 3).

We followed this analysis with an evaluation of the role of IRF4 in the decidualization. HESCs were transfected with scrambled (siNT) and IRF4-targeting (siIRF4) siRNA. After 6 days of hormone stimulus, HESCs transfected with siNT displayed a decidual, cobblestone morphology. HESCs transfected with siIRF4 displayed fibroblastic cell morphology indicative of an absent decidual transformation (Figure 6A). Gene expression analysis by RT-qPCR indicated that the significant ablation of *IRF4* through the decidualization process did not affect the expression of *PR* and only attenuated the expression of *FOXO1* at day 6. However, in siIRF4-treated HESC expression of the decidual markers *IGFBP1*, *PRL*, and *WNT4* were significantly attenuated on both days 3 and 6. These gene expression changes are consistent with the observation

that siIRF4-treated HESCs did not undergo a morphological decidual transformation. Overall, these results identify, for the first time, the role of IRF4 in HESC differentiation.

Discussion

In this study we described the global genomic binding landscape of FOXO1 and the FOXO1-dependent transcriptome in human endometrial stromal cells after 3 days of stimulation with 17β-estradiol, medroxyprogesterone acetate, and cAMP. In a comparison of the transcriptome of HESCs in decidualization (vehicle and EPC) with the transcriptome of HESCs transfected with siFOXO1, we observed that more than half of the genes differentially regulated in siFOXO1 were actively regulated in decidualization. We subsequently focused solely on genes that were being actively transcribed at this time, as indicated by the occupancy of RNApol II, and we identified 437 genes. These genes were involved in pathways known to be critical for the differentiation of HESCs because they were effectors of the morphological transformation underlying changes in focal adhesions, cell cycle, and ECM receptor interaction (32–34). Moreover, we observed a predominance of genes involved in several cancers, including prostate, colorectal, leukemia, and small-cell lung cancer. Gene ontology analysis also revealed enrichments in the regulation of cell proliferation and cell death, pathways deregulated in endometrial carcinoma, and endometriosis in which FOXO1 expression is significantly down-regulated (35, 36).

To identify direct genomic targets of FOXO1, we performed ChIP-seq for FOXO1 in HESCs after 72 hours of EPC treatment. It has been reported that the expression of FOXO1 is induced after 2 days of cAMP and progestin stimulation and peaks at day 6 of decidualization. Interestingly, studies have shown that by day 4 most of FOXO1 is phosphorylated and exported from the nucleus (37). The predominantly cytoplasmic localization of FOXO1 is tightly regulated and is dependent on sustained progestin stimulation and activation of the phosphatidyl-inositol 3-kinase/AKT pathway (38). There is evidence to suggest that the residual nuclear pool of FOXO1 is essential and sufficient to have a significant role in the regulation of decidual gene transcription (14). By confocal immunofluorescence imaging, we determined a significant FOXO1 presence in the nucleus of decidual HESCs. Western blot analysis of nuclear and cytoplasmic fractions was consistent with previous evidence in demonstrating that although most FOXO1 was found in the cytoplasmic fraction, a residual portion of FOXO1 was
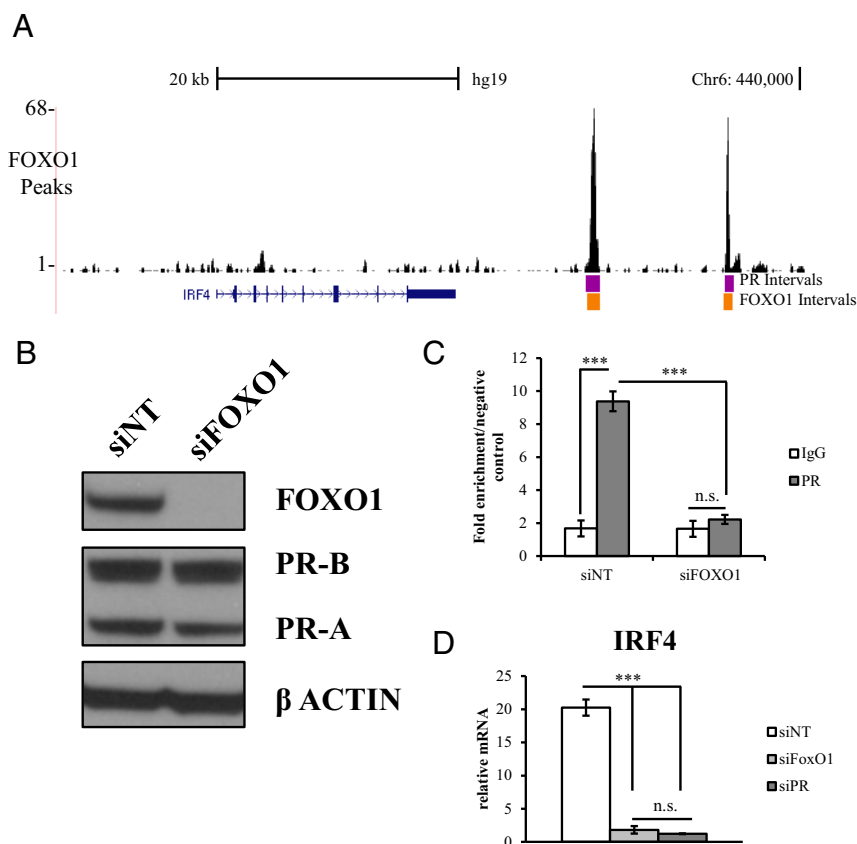
Figure 5. FOXO1 and PR regulation of IRF4. A, University of California, Santa Cruz genome browser snapshot of PR and FOXO1 intervals downstream of the *IRF4* gene. B, Western blot analysis of PR and FOXO1 protein expression in HESCs transfected with scrambled (siNT) siRNA and FOXO1 targeting (siFOXO1) siRNA prior to EPC treatment. C, ChIP-qPCR validation of FOXO1 and PR binding on the downstream ChIP-seq binding intervals in HESCs treated with scrambled siRNA (siNT) or targeting siRNA (siFOXO1) prior to decidual stimulus. Data are represented as fold enrichment of IgG and PR over that of the negative control region in a gene desert on chromosome 4. n.s., not significant ($P > .05$). ∗∗∗, $P < .001$. D, Gene expression validation by RT-qPCR of *IRF4* in HESCs after siRNA-mediated silencing of FOXO1 or PR. Expression data for *IRF4* were normalized to that of 18s rRNA. Data are based on three independent experiments. Error bars represent SEM. n.s., not significant ($P > .05$). ∗∗∗, $P < .001$.

present in the nucleus, thereby able to engage in the regulation of transcription.

ChIP-seq analysis revealed that FOXO1 has a large amount of binding sites throughout the genome and does not show a clear preference for particular genomic regions. However, when we evaluated only the intervals near genes we found to be differentially regulated after silencing of *FOXO1* (2760 intervals), CEAS revealed enrichment in the promoter region (2000–3000 bp) and 5′UTR. This evidence suggests that although FOXO1 may be interacting widely across the genome, binding of FOXO1 is predominantly found near the regulatory elements in promoters of genes regulated by this transcription factor. It is hypothesized that FOXO1 exhibits a proapoptotic role in the absence of progestin and that this mechanism is functionally required for the execution of decidual regression for the cyclic regeneration of the endometrium

(39). It remains to be determined whether the cistrome of FOXO1 in HESCs changes after progestin withdrawal when the cytoplasmic pool of FOXO1 becomes nuclear and how this change affects the FOXO1-dependent transcriptome.

Among the direct targets of FOXO1 was *IGF-1*. IGF-1, like other growth factors expressed in differentiating HESCs, can activate phosphatidylinositol 3-kinase/AKT pathways. *IGF-1* expression and MAPK3/1 activation is observed in normal proliferative-phase endometrium. In endometrial carcinoma, estrogen-induced proliferation is mediated by the MAPK3/1 pathway via autocrine stimulation of IGF-1 (40, 41). *IGF-1* was enriched in the pathway annotation of siFOXO1-regulated genes under several categories including cancer, focal adhesion, and p53 signaling. The regulation of *IGF-1* by FOXO1 may function in a negative regulatory loop that contributes to the mechanism by which phosphorylation and cytoplasmic retention of FOXO1 is regulated during decidualization. These observations highlight the important role of IGF-1 in the decidualization processes, particularly in the regulation of the balance that favors survival over apoptosis.

Forkhead box proteins interact directly with chromatin by binding to forkhead response elements on DNA and function as pioneer factors and/or classical transcription factors to recruit coactivators or other transcription factors (42). Motif analysis of the FOXO1-binding intervals revealed an enrichment of motifs recognized by the forkhead domain family. Among the top enriched motifs were also those recognized by the Runt domain family, represented by Runt-related transcription (RUNX)-factor 1. The RUNX family of genes form heterodimeric complexes with other core-binding factors on promoters and enhancers and confers increased DNA binding and stability to the complex. RUNX family members are involved in several cellular processes, including development and differentiation and have been shown to integrate oncogenic signals or environmental cues for the regulation of tumor-suppressive responses (43, 44).
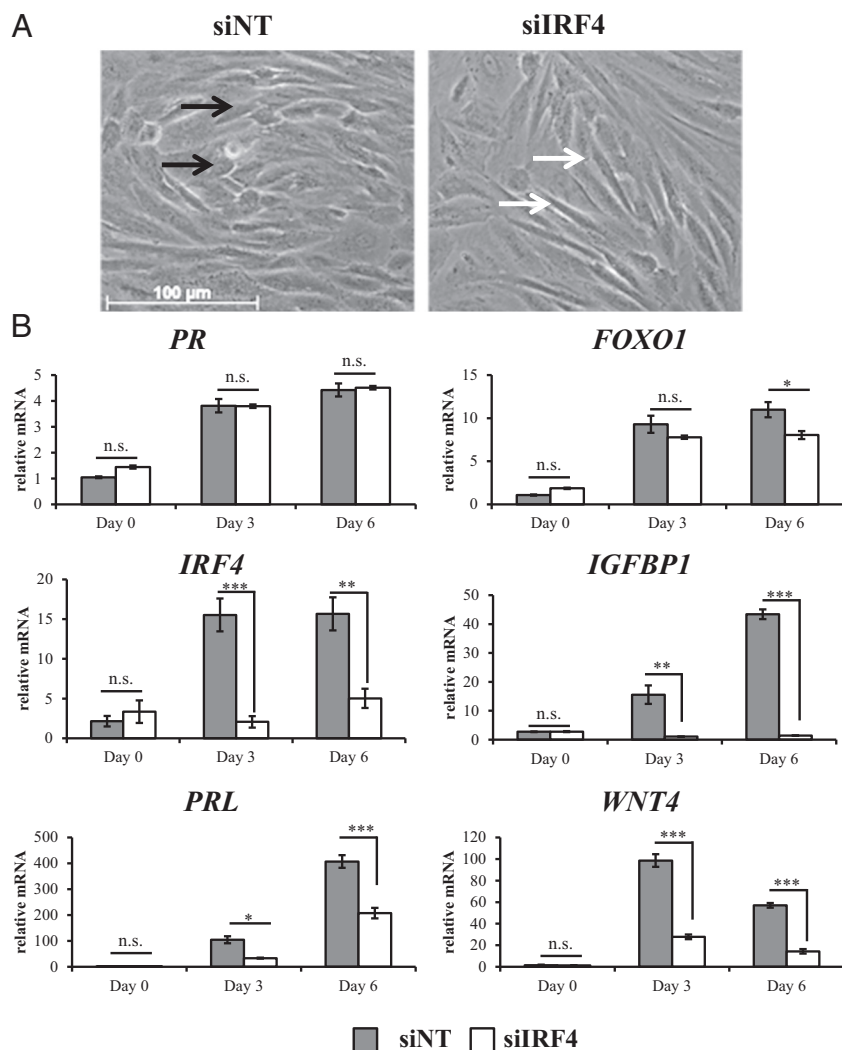
Figure 6. Requirement of IRF4 for the in vitro decidualization of HESCs. A, Micrographs for cells treated with scrambled siRNA (siNT) or targeting siRNA (siIRF4). Black arrows indicate decidual cells, and white arrows indicate fibroblastic (nondecidual) stromal cells. B, Gene expression validation by RT-qPCR of *PGR*, *FOXO1*, *IRF4*, *IGFBP1*, *PRL*, and *WNT4* in HESCs transfected with scrambled siRNA (siNT) or targeting siRNA (siIRF4) prior to EPC treatment for 0, 3, and 6 days. Expression data for each gene were normalized to that of 18s rRNA. Data are based on three independent experiments. Error bars represent SEM. *, $P < 0.05$; **, $P < .01$; ***, $P < .001$.

ulation of *RUNX1* may be a novel mechanism by which FOXO1 regulates changes in proliferation in the differentiation of HESCs.

Although significant evidence has been presented for the physical interaction of FOXO1 and PR, the nature of the direct or indirect interaction, through association of other cofactors, remained unclear. To evaluate these potential interactions, we generated intervals of co-occupancy of FOXO1 and PR. These intervals contained a significant enrichment in progesterone response elements and forkhead response elements. It was hypothesized that the interaction of PR with other cAMP-induced transcription factors allowed PR to regulate genes that were devoid of PRE (14). However, the high enrichment of hormone response elements (HRE) in these co-occupied genomic regions suggests that the absence of hormone response elements may not necessarily be the reason for the transcriptional cross talk between PR and other factors. Instead, the requirement for other factors to be recruited to these regulatory regions may have alternative functions in transcription activation or repression. FOXO1, like other members of the Forkhead domain family, has been described as pioneer factor in several cellular contexts. As pioneer factors, FOX

RUNX1 also plays a role in neoplastic transformation of endometrioid carcinomas (45). The role of RUNX1 in decidualization has never been evaluated. We observed that *RUNX1* is down-regulated with EPC treatment of HESCs, and the absence of FOXO1 disrupts this down-regulation. FOXO1 had numerous binding sites throughout the gene body during HESC decidualization, suggesting that FOXO1 may have a direct role in the inhibition of transcriptional elongation of *RUNX1*. The requirement of the down-regulation of *RUNX1* for the proper differentiation of HESCs remains to be determined. Previously it was reported that silencing FOXO1 promoted the proliferation of differentiating HESCs due to its ability to regulate the expression of many cell cycle regulators, among them *CCNB1*, *CCNB2*, *MCM5*, and *CDC2* (14). The FOXO1-dependent down-reg-

proteins can associate with compacted chromatin and modulate chromatin to facilitate accessibility for other transcription factors (42). In this study, we presented evidence for the requirement of FOXO1 for the binding of PR to DNA on the common target genes. The observed decrease in PR enrichment at these genomic locations after the silencing FOXO1 was not due to changes in PR isoform protein expression but may be attributed to the decrease in the chromatin accessibility for PR.

We also observed an enrichment of ISRE in the co-occupied PR/FOXO1 intervals, which led us to hypothesize a role for IRF4 in the transcriptional regulation in decidualization. The function of the interferon regulatory factors in endometrial biology has only been superficially explored. The expression of several members including *IRF1* and *IRF2* has been shown in the secretory phase of menstrual

cycle in humans and in the ovine endometrium (46, 47). *IRF4* is expressed in most cell types of the immune system and is essential for the development and function of T helper cells, regulatory T cells, B cells, and dendritic cells (48). *IRF4* is induced by mitogenic stimulus and type I interferon. Interferon regulatory factor members are involved in the regulation of the cell cycle and apoptosis in innate and adaptive immune responses and oncogenesis (49, 50). In CD4(+) T cells, IRF4 regulates the expression of the cytokine IL-10 in response to pathogens (51). IL-10 and its receptor are significantly expressed in the cycling endometrium, and some studies report their expression significantly increases in decidual cultures (52). IL-10, along with a multitude of other cytokines, plays a critical role in the regulation of maternal tolerance to the fetal allograft, and one of the critical functions of the decidua is to modulate the cytokine section at the fetal-maternal interphase.

We had previously demonstrated how the hormonal regulation of cytokine signaling in decidualization is mediated by the chicken ovalbumin upstream promoter-transcription factor II (NR2F2). Motif analysis of the chicken ovalbumin upstream promoter-transcription factor II DNA-binding intervals revealed an enrichment in FOXO1 motifs (29). The role of IRF4 in the modulation of inflammation and immune response in differentiating HESCs remains to be determined. In this study we identified a novel role of IRF4 in HESC differentiation by demonstrating that siRNA-mediated silencing of IRF4 significantly attenuated the expression of all decidual marker genes evaluated, with the exception of FOXO1 at day 3. The attenuation of IRF4 did not affect the expression of PR, suggesting that it is downstream of progesterone signaling. Overall, this evidence suggests IRF4 as a novel transcriptional coregulator of FOXO1 and PR in HESC differentiation.

In summary, this study investigated the cistrome and transcriptome of FOXO1 in the differentiation of HESCs and identified many direct target genes involved in previously reported pathways such as cell cycle and apoptosis. We identified numerous binding locations for FOXO1 across the genome and determined that more than half of the genes regulated with siRNA-mediated knockdown of FOXO1 are bound near their promoter regions. We identified numerous binding elements within the FOXO1-binding intervals recognized by known transcriptional coregulators of FOXO1, including HOX and CEBP, and novel putative partners, including RUNX1 and IRF4. Furthermore, we established the high co-occupancy of FOXO1 in PR binding across the genome during decidualization. Finally, we established the requirement of FOXO1 for the binding of PR to a novel target gene and putative regulator of decidualization, IRF4.

References

1. **Gellersen B, Brosens IA, Brosens JJ.** Decidualization of the human endometrium: mechanisms, functions, and clinical perspectives. *Semin Reprod Med.* 2007;25:445–453.
2. **Brar AK, Handwerger S, Kessler CA, Aronow BJ.** Gene induction and categorical reprogramming during in vitro human endometrial fibroblast decidualization. *Physiol Genomics.* 2001;7:135–148.
3. **Warning JC, McCracken SA, Morris JM.** A balancing act: mechanisms by which the fetus avoids rejection by the maternal immune system. *Reproduction.* 2011;141:715–724.
4. **Cha J, Sun X, Dey SK.** Mechanisms of implantation: strategies for successful pregnancy. *Nat Med.* 2012;18:1754–1767.
5. **Cloke B, Huhtinen K, Fusi L, et al.** The androgen and progesterone receptors regulate distinct gene networks and cellular functions in decidualizing endometrium. *Endocrinology.* 2008;149:4462–4474.
6. **Lydon JP, DeMayo FJ, Funk CR, et al.** Mice lacking progesterone receptor exhibit pleiotropic reproductive abnormalities. *Genes Dev.* 1995;9:2266–2278.
7. **Rowan BG, Garrison N, Weigel NL, O'Malley BW.** 8-Bromo-cyclic AMP induces phosphorylation of two sites in SRC-1 that facilitate ligand-independent activation of the chicken progesterone receptor and are critical for functional cooperation between SRC-1 and CREB binding protein. *Mol Cell Biol.* 2000;20:8720–8730.
8. **Wagner BL, Norris JD, Knotts TA, Weigel NL, McDonnell DP.** The nuclear corepressors NCoR and SMRT are key regulators of both ligand- and 8-bromo-cyclic AMP-dependent transcriptional activity of the human progesterone receptor. *Mol Cell Biol.* 1998;18:1369–1378.
9. **Jones MC, Fusi L, Higham JH, et al.** Regulation of the SUMO pathway sensitizes differentiating human endometrial stromal cells to progesterone. *Proc Natl Acad Sci USA.* 2006;103:16272–16277.
10. **Gellersen B, Brosens J.** Cyclic AMP and progesterone receptor cross-talk in human endometrium: a decidualizing affair. *J Endocrinol.* 2003;178:357–372.
11. **Huang H, Tindall DJ.** Dynamic FoxO transcription factors. *J Cell Sci.* 2007;120:2479–2487.
12. **Kajihara T, Brosens JJ, Ishihara O.** The role of FOXO1 in the decidual transformation of the endometrium and early pregnancy. *Med Mol Morphol.* 2013;46:61–68.
13. **Buzzio OL, Lu Z, Miller CD, Unterman TG, Kim JJ.** FOXO1A differentially regulates genes of decidualization. *Endocrinology.* 2006;147:3870–3876.
14. **Takano M, Lu Z, Goto T, et al.** Transcriptional cross talk between the

forkhead transcription factor forkhead box O1A and the progesterone receptor coordinates cell cycle regulation and differentiation in human endometrial stromal cells. *Mol Endocrinol.* 2007;21:2334–2349.

15. **Lynch VJ, Brayer K, Gellersen B, Wagner GP.** HoxA-11 and FOXO1A cooperate to regulate decidual prolactin expression: towards inferring the core transcriptional regulators of decidual genes. *PLoS One.* 2009;4:e6845.

16. **Christian M, Zhang X, Schneider-Merck T, et al.** Cyclic AMP-induced forkhead transcription factor, FKHR, cooperates with CCAAT/enhancer-binding protein β in differentiating human endometrial stromal cells. *J Biol Chem.* 2002;277:20825–20832.

17. **Ghosh AK, Lacson R, Liu P, et al.** A nucleoprotein complex containing CCAAT/enhancer-binding protein β interacts with an insulin response sequence in the insulin-like growth factor-binding protein-1 gene and contributes to insulin-regulated gene expression. *J Biol Chem.* 2001;276:8507–8515.

18. **Kim JJ, Taylor HS, Akbas GE, et al.** Regulation of insulin-like growth factor binding protein-1 promoter activity by FKHR and HOXA10 in primate endometrial cells. *Biol Reprod.* 2003;68:24–30.

19. **Kim JJ, Buzzio OL, Li S, Lu Z.** Role of FOXO1A in the regulation of insulin-like growth factor-binding protein-1 in human endometrial cells: interaction with progesterone receptor. *Biol Reprod.* 2005;73:833–839.

20. **Brosens JJ, Hayashi N, White JO.** Progesterone receptor regulates decidual prolactin expression in differentiating human endometrial stromal cells. *Endocrinology.* 1999;140:4809–4820.

21. **Gellersen B, Brosens JJ.** Cyclic decidualization of the human endometrium in reproductive health and failure. *Endocr Rev.* 2014; 35(6):851–905.

22. **Cakmak H, Taylor HS.** Implantation failure: molecular mechanisms and clinical treatment. *Hum Reprod Update.* 2011;17:242–253.

23. **Spandidos A, Wang X, Wang H, Seed B.** PrimerBank: a resource of human and mouse PCR primer pairs for gene expression detection and quantification. *Nucleic Acids Res.* 2010;38:D792–D799.

24. **Langmead B, Trapnell C, Pop M, Salzberg SL.** Ultrafast and memory-efficient alignment of short DNA sequences to the human genome. *Genome Biol.* 2009;10:R25.

25. **Trapnell C, Pachter L, Salzberg SL.** TopHat: discovering splice junctions with RNA-Seq. *Bioinformatics.* 2009;25:1105–1111.

26. **Parkhomchuk D, Borodina T, Amstislavskiy V, et al.** Transcriptome analysis by strand-specific sequencing of complementary DNA. *Nucleic Acids Res.* 2009;37:e123.

27. **Robinson MD, McCarthy DJ, Smyth GK.** edgeR: a Bioconductor package for differential expression analysis of digital gene expression data. *Bioinformatics.* 2010;26:139–140.

28. **Rubel CA, Lanz RB, Kommagani R, et al.** Research resource: genome-wide profiling of progesterone receptor binding in the mouse uterus. *Mol Endocrinol.* 2012;26:1428–1442.

29. **Li X, Large MJ, Creighton CJ, et al.** COUP-TFII regulates human endometrial stromal genes involved in inflammation. *Mol Endocrinol.* 2013;27:2041–2054.

30. **Liu T, Ortiz JA, Taing L, et al.** Cistrome: an integrative platform for transcriptional regulation studies. *Genome Biol.* 2011;12:R83.

31. **Huang da W, Sherman BT, Lempicki RA.** Systematic and integrative analysis of large gene lists using DAVID bioinformatics resources. *Nat Protoc.* 2009;4:44–57.

32. **Shiokawa S, Yoshimura Y, Nagamatsu S, et al.** Functional role of focal adhesion kinase in the process of implantation. *Mol Hum Reprod.* 1998;4:907–914.

33. **Das SK.** Cell cycle regulatory control for uterine stromal cell decidualization in implantation. *Reproduction.* 2009;137:889–899.

34. **Reddy KV, Mangale SS.** Integrin receptors: the dynamic modulators of endometrial function. *Tissue Cell.* 2003;35:260–273.

35. **Ward EC, Hoekstra AV, Blok LJ, et al.** The regulation and function of the forkhead transcription factor, Forkhead box O1, is dependent on the progesterone receptor in endometrial carcinoma. *Endocrinology.* 2008;149:1942–1950.

36. **Shazand K, Baban S, Prive C, et al.** FOXO1 and c-jun transcription factors mRNA are modulated in endometriosis. *Mol Hum Reprod.* 2004;10:871–877.

37. **Grinius L, Kessler C, Schroeder J, Handwerger S.** Forkhead transcription factor FOXO1A is critical for induction of human decidualization. *J Endocrinol.* 2006;189:179–187.

38. **Labied S, Kajihara T, Madureira PA, et al.** Progestins regulate the expression and activity of the forkhead transcription factor FOXO1 in differentiating human endometrium. *Mol Endocrinol.* 2006;20:35–44.

39. **Brosens JJ, Gellersen B.** Death or survival—progesterone-dependent cell fate decisions in the human endometrial stroma. *J Mol Endocrinol.* 2006;36:389–398.

40. **Kashima H, Shiozawa T, Miyamoto T, et al.** Autocrine stimulation of IGF1 in estrogen-induced growth of endometrial carcinoma cells: involvement of the mitogen-activated protein kinase pathway followed by up-regulation of cyclin D1 and cyclin E. *Endocr Relat Cancer.* 2009;16:113–122.

41. **Giudice LC, Dsupin BA, Jin IH, Vu TH, Hoffman AR.** Differential expression of messenger ribonucleic acids encoding insulin-like growth factors and their receptors in human uterine endometrium and decidua. *J Clin Endocrinol Metab.* 1993;76:1115–1122.

42. **Lam EW, Brosens JJ, Gomes AR, Koo CY.** Forkhead box proteins: tuning forks for transcriptional harmony. *Nat Rev Cancer.* 2013;13:482–495.

43. **Chuang LS, Ito K, Ito Y.** RUNX family: regulation and diversification of roles through interacting proteins. *Int J Cancer.* 2013;132:1260–1271.

44. **Ozaki T, Nakagawara A, Nagase H.** RUNX family participates in the regulation of p53-dependent DNA damage response. *Int J Genomics.* 2013;2013:271347.

45. **de Sousa VP, Chaves CB, Huguenin JF, et al.** ERM/ETV5 and RUNX1/AML1 expression in endometrioid adenocarcinomas of endometrium and association with neoplastic progression. *Cancer Biol Ther.* 2014;15:888–894.

46. **Jabbour HN, Critchley HO, Yu-Lee LY, Boddy SC.** Localization of interferon regulatory factor-1 (IRF-1) in nonpregnant human endometrium: expression of IRF-1 is up-regulated by prolactin during the secretory phase of the menstrual cycle. *J Clin Endocrinol Metab.* 1999;84:4260–4265.

47. **Spencer TE, Ott TL, Bazer FW.** Expression of interferon regulatory factors one and two in the ovine endometrium: effects of pregnancy and ovine interferon tau. *Biol Reprod.* 1998;58:1154–1162.

48. **Xu WD, Pan HF, Ye DQ, Xu Y.** Targeting IRF4 in autoimmune diseases. *Autoimmun Rev.* 2012;11:918–924.

49. **Taniguchi T, Ogasawara K, Takaoka A, Tanaka N.** IRF family of transcription factors as regulators of host defense. *Annu Rev Immunol.* 2001;19:623–655.

50. **Tamura T, Yanai H, Savitsky D, Taniguchi T.** The IRF family transcription factors in immunity and oncogenesis. *Annu Rev Immunol.* 2008;26:535–584.

51. **Lee CG, Hwang W, Maeng KE, et al.** IRF4 regulates IL-10 gene expression in CD4(+) T cells through differential nuclear translocation. *Cell Immunol.* 2011;268:97–104.

52. **Vigano P, Somigliana E, Mangioni S, Vignali M, Di Blasio AM.** Expression of interleukin-10 and its receptor is up-regulated in early pregnant versus cycling human endometrium. *J Clin Endocrinol Metab.* 2002;87:5730–5736.